Astron. Astrophys. 359, 159–167 (2000)

ASTRONOMY AND ASTROPHYSICS

Rotational modulation and flares on RS CVn and BY Dra stars

XX. Photometry and spectroscopy of CC Eri in late 1989

P.J. Amado[1,⋆], J.G. Doyle[1], P.B. Byrne[⋆⋆], G. Cutispoto[2], D. Kilkenny[3], M. Mathioudakis[4], and J.E. Neff[5]

[1] Armagh Observatory, College Hill, Armagh BT61 9DG, Ireland
[2] Catania Astrophysical Observatory, Viale A. Doria, 6. 95125 Catania, Italy
[3] South African Astronomical Observatory, P.O. Box 7, Observatory 7935, South Africa
[4] Queens University of Belfast, Department of Pure and Applied Physics, Belfast BT7 1NN, Ireland
[5] College of Charleston, Department of Physics and Astronomy, Charleston, SC 29424, USA

Received 12 November 1999 / Accepted 14 April 2000

Abstract. The active flaring binary CC Eri was studied via multi-wavelength observations involving multi-based photometry and ground- and space-based spectroscopy. Combining early spectroscopic data with the present implies an orbital period of $P = 1.5615$ days. Furthermore, the spectroscopic data suggests spectral types of K7 and M3 for the system. The optical photometry indicated a small spot coverage in late 1989, consistent with data taken a year later which showed CC Eri entering its brightest-to-date phase.

Two flares were detected in the ultraviolet spectral data. These flares radiated $2.7\,10^{31}$ erg and $1.6\,10^{31}$ erg in the C IV line alone, each with a total estimated radiative energy budget of $\approx 10^{36}$ erg. For the higher-temperature lines, such as C IV, there was no systematic variability with phase. The lower-temperature lines show a slight indication of rotational modulation. However, there is a much larger scatter in the individual measurements of the Mg II and C IV fluxes than would be expected from measurement errors alone, consistent with an atmosphere showing continual small-scale activity.

Key words: stars: activity – stars: binaries: spectroscopic – stars: chromospheres – stars: individual: CC Eri – stars: late-type – ultraviolet: stars

1. Introduction

CC Eri (= HD16157 = CD$-44°775$ = GJ 103) is a 1.56 day spectroscopic binary with a mass ratio of ≈2 (Evans 1959). The primary is a K7Ve and co-rotates with the orbital motion, as shown by its light variations (Bopp & Evans 1973). As such, it is one of the most rapidly rotating late K solar neighbourhood dwarfs known. Others include, YY Gem (= GJ 278c, 0.8 day) and HK Aqr (= GJ 890, 0.4 day), although several ultra-fast rotators are known to exist within the local association (e.g. see Jefferies et al. 1994 and references therein).

CC Eri is a known flare star whose activity rate is at a level of a ΔU=1 mag flare every ≈12 hr (Busko & Torres 1976). CC Eri has been observed with the VLA, resulting in 6 cm flux measurements of 0.62 ± 0.08 mJy and 1.34 mJy (Caillault et al. 1988) and ≤ 0.23 mJy (White et al. 1994). It is also an infrared source with a luminosity of $\sim 2.2\,10^{30}$ erg s^{-1} at 12 μm (Tsikoudi 1988). In spite of its many interesting properties, CC Eri is a relatively neglected object and had only a single ultraviolet spectrum taken prior to the present data. This spectrum, in the IUE long wavelength spectral region (1900–3200 Å) yielded a Mg II resonance line luminosity that indicated a very high level of chromospheric heating (Byrne et al. 1982). It is also a powerful X-ray source, having been measured with Einstein (Schmitt et al. 1987), EXOSAT (Pallavicini et al. 1988, 1990) and ROSAT (Pan & Jordan 1995), yielding X-ray luminosities between $\log L_{\rm X} = 29.2$ and 29.8 erg s^{-1}.

In this paper we report on simultaneous optical and ultraviolet spectroscopy plus photometry of CC Eri taken in November 1989. Based on these data we examine the orbital solution of the binary system and discuss the energy balance in the star's magnetically heated chromosphere and transition region, in both quiescent and flaring conditions. The ultraviolet data was supplemented with more recent data from the extreme ultraviolet region. We also examine the evidence for rotational modulation in the optical and ultraviolet line emission. Preliminary results were given by Byrne et al. (1992).

2. Observational data

2.1. Photometry

The optical photometry was carried out on the 1.0m telescope at the South African Astronomical Observatory at Sutherland during October/November 1989 and at the European Southern Observatory's 0.5m telescope at La Silla during December 1989.

Send offprint requests to: P.J. Amado

⋆ *Present address:* Instituto de Astrofísica de Andalucía-CSIC, Apartado 3004, 18080 Granada, Spain (pja@iaa.es)

⋆⋆ Deceased

Table 1. *UBV(RI)*$_c$ photometry from the South African Astronomical Observatory (SAAO) and the European Southern Observatory (ESO). Mean magnitudes and colours for the local comparisons used are also given. Phases are according to the ephemeris $2\,447\,129.5293 + 1.56145E$.

SAAO

HJD(2 440 000+)	Phase	V	U–B	B–V	V–R	V–I	Comment
7834.2990	0.3559	8.756	0.969	1.362	0.894	1.819	Flare?
7834.4640	0.4616	8.775	1.098	1.372	0.898	1.829	
7834.5780	0.5346	8.776	1.097	1.370	0.897	1.826	
7835.3000	0.9970	8.751	1.121	1.375	0.892	1.814	
7836.3010	0.6380	8.768	1.110	1.377	0.895	1.816	
7836.4360	0.7245	8.764	1.116	1.380	0.896	1.820	
7837.2890	0.2708	8.780	1.100	1.380	0.893	1.820	
7849.2970	0.9611	8.746	1.078	1.373	0.893	1.813	
7849.5380	0.1154	8.764	1.130	1.371	0.894	1.822	
7850.4880	0.7238	8.752	1.104	1.372	0.892	1.813	
7851.3000	0.2439	8.769	1.070	1.376	0.893	1.820	

HD15567: V=8.695, (B–V)=1.597, (U–B)=1.952, (V–R)$_c$=0.934, (V–I)$_c$=1.963
HD16651: V=8.132, (B–V)=1.167, (U–B)=1.064, (V–R)$_c$=0.596, (V–I)$_c$=1.144

ESO

HJD(2 440 000+)	Phase	V	U–B	B–V	V–R	V–I	Comment
7869.6730	0.0105	8.741	1.128	1.372	0.870	1.805	
7870.6610	0.6432	8.748	1.116	1.373	0.868	1.814	
7872.6280	0.9029	8.735	1.117	1.364	0.870	1.810	
7873.6510	0.5581	8.762	1.144	1.370	0.867	1.816	
7874.6501	0.1980	8.761	1.131	1.380	0.867	1.811	
7876.6824	0.4995	8.774	1.132	1.390	0.872	1.823	
7878.6744	0.7752	8.745	1.115	1.375	0.865	1.815	
7879.5957	0.3653	8.767	——	1.384	0.873	1.819	No U-band mesured
7882.6313	0.3094	8.762	1.132	1.376	0.873	1.811	
7885.6437	0.2386	8.759	1.127	1.378	0.866	1.811	
7888.5520	0.1012	8.759	1.136	1.372	0.879	1.818	
7888.6186	0.1438	8.764	1.136	1.373	0.876	1.814	
7888.6603	0.1705	8.764	1.132	1.374	0.871	1.813	

HD16371: V=8.09, (B–V)=0.90, (U–B)=0.57, (V–R)$_c$=0.47, (V–I)$_c$=0.92
SAO215945: V=9.73, (B–V)=0.39, (U–B)=-0.01, (V–R)$_c$=0.22, (V–I)$_c$=0.44

2.1.1. Photometry–European Southern Observatory

The observations of CC Eri (v = variable star) at the ESO were carried out over the period 9–28 December 1989 using a 0.5m telescope equipped with a single-channel photon-counting photometer, a thermoelectrically cooled RCA 31034 GaAs photomultiplier and standard ESO filters matching the *UBV(RI)*$_c$ system. HD 16371 and SAO 215945 were used as comparison (c) and check (ck) star, respectively. Each measurement of a star consisted of 10–15 1-sec integrations in each filter, according to the *U–B–V–R*$_c$*–I*$_c$ colour sequence. A complete observation consisted of sequential *c-v-v-v-ck-c* measurements. From these data, after accurate sky subtraction, three *v-c* and one *ck-c* differential magnitudes were computed; the three *v-c* values were finally averaged to obtain one data point. The observations were corrected for atmospheric extinction and transformed into the standard *UBV(RI)*$_c$ system. The typical data point error for the differential photometry is of the order of 0.005 magnitudes, with somewhat larger values in the U-band due to the low photon counting level. The accuracy of the absolute photometry is of the order of 0.01 magnitudes (see Cutispoto 1995 for further details).

2.1.2. Photometry–South African Astronomical Observatory

The SAAO data were obtained between 3–10 November 1989 with the 1.0m telescope and the St. Andrews photoelectric photometer. CC Eri was observed together with local comparison stars HD 15567 and 16651, and reduction of the *UBV(RI)*$_c$ observations was carried out using E-region standard stars from the compilation given by Menzies et al. (1989) and conventional SAAO reduction procedures. Mean values for the local comparisons are given in Table 1 and were used to differentially correct the CC Eri data.

2.2. Optical spectroscopy

CC Eri was observed with the University College London Echelle Spectrograph (UCLES) on the Anglo-Australian Tele-

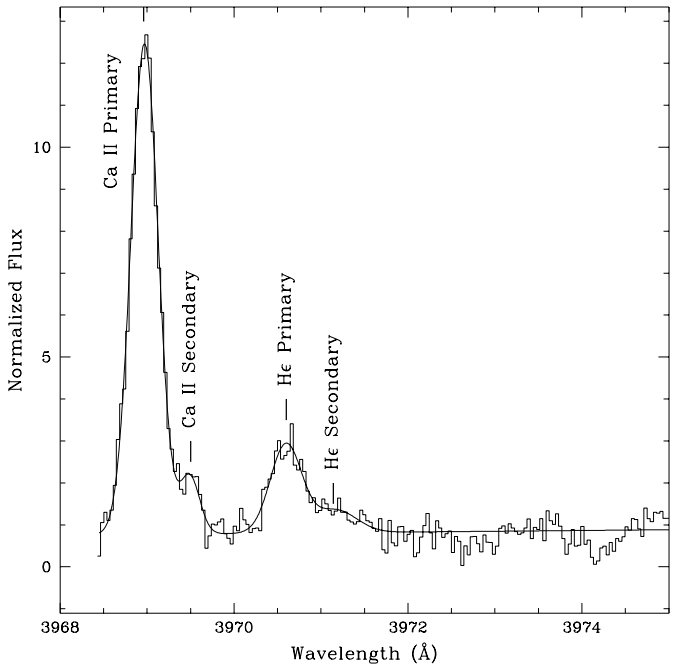

Fig. 1. An example of spectra taken with the UCLES on the Anglo Australian Telescope in the region of Ca II H and Hϵ. A 4-gaussian fit plus continuum is also shown, where the centres of the gaussians are indicated by dashes.

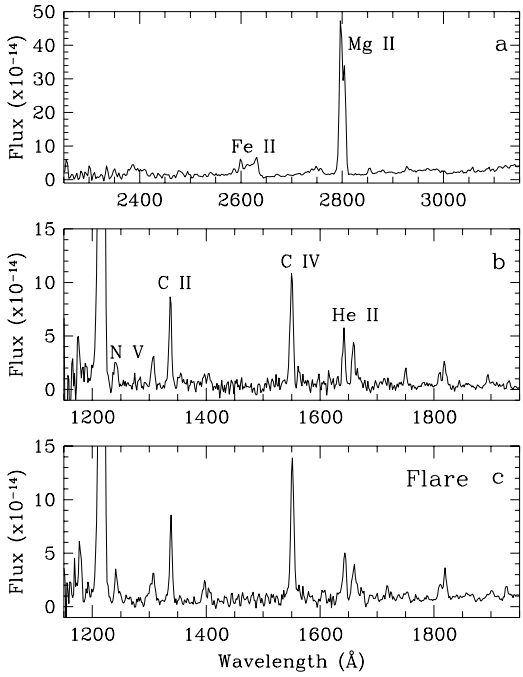

Fig. 2. a Mean LWP and **b** SWP IUE spectrum of CC Eri outside of flaring and **c** SWP spectrum of the flare event on 4 November.

scope (AAT). The UCLES was equipped with a 31.6 grooves mm^{-1} echelle grating and a GEC CCD (256×584 pxl) which give an effective resolution of R$\sim$ 55 000. The spectra covered a number of non-contiguous spectral regions from $\sim$3860 Å to $\sim$4165 Å. Data were obtained on three consecutive nights 2–4 November 1989 but clouds affected all three nights at some time during the observations. An exposure time of two minutes was set for all the spectra, which were obtained whenever sky conditions allowed in a continuous cycling mode. This observing strategy was adopted to ensure good discrimination against short-lived flare events, although it gave a low signal-to-noise ratio, which made it difficult to measure the photospheric absorption lines.

The data were reduced using the astronomical computing environment, IRAF (Tody et al. 1986), available on the UK STARLINK astronomical computing network (Bromage 1984). A sample spectrum in the region of the Ca II H/Hϵ chromospheric emission lines is presented in Fig. 1, where gaussians were used to produce the fit shown in the figure as a solid line. The binary nature of the star can be clearly seen from the doubling of the emission lines.

2.3. UV spectroscopy

CC Eri was observed on the 2, 3 and 4 November 1989 using the UV spectrograph on board the International Ultraviolet Explorer (IUE) satellite with both the long (LWP; 1900–3200 Å) and short (SWP; 1150–1950 Å) wavelength cameras. The star was moved between two positions at either end of the spectrograph slit thus yielding two spectra per image. This was done to maximise the amount of data collected since the spacecraft readout overhead was comparable to the exposure time. A further efficiency was gained by alternating long and short wavelength spectra, in such a way that one camera was exposing while the other was being read. A full log of the IUE spectra will be found in Tables 2 and 3. The spectra were extracted and flux calibrated from the IUE images using the program IUEDR (Giddings 1983). They were then subjected to a light gaussian smoothing procedure using the program DIPSO (Howarth & Murray 1988). This smoothing was such as to be consistent with the known resolution of the spectrograph. An example of the smoothed spectra is shown in Fig. 2, where emission lines are identified. Their fluxes were determined by fitting gaussian profiles, again using DIPSO, by a least-squares measure of the goodness of the fit. Where lines were blended, multiple gaussians were used. The resulting line fluxes are found in Tables 2 and 3.

The spectra in Fig. 2 show a number of emission lines typical of active stars, including, in the LWP region, the Mg II h and k ($\lambda\lambda$ 2796/2803 Å) and the strong Fe II lines near λ2600 Å and, in the SWP region, the C IV ($\lambda\lambda$1548/1551 Å), C II ($\lambda\lambda$1335/1336 Å) and He II (λ1640 Å) lines. As can be seen in the lower panel of Fig. 2, in addition to a greatly increased C IV line emission, there is a sizeable continuum flux in the SWP spectra SWP37513B, indicating a large flaring event. Details on the line fluxes of this flare and another two are given in Table 4, where the fluxes have been computed by subtracting the mean flux for each day (without the flares, in Table 2) from the total flux measured in the lines.

Table 2. IUE SWP emission line fluxes at Earth for CC Eri between 2–4 November 1989. A mean flux and associated variances are given for each line on each date. A second mean is given in brackets, where appropriate, which excludes those points flagged as flares in the Comments column. Phases are according to the ephemeris $2\,447\,129.5293 + 1.56145E$. The notation JD2, JD3 and JD4 refer to data taken on 2 Nov., 3 Nov. and 4 Nov. respectively.

IUE Image Number	JD 2 447 830.0+	Phase	Line Flux ($\times 10^{-13}$ erg s^{-1} cm^{-2}) N V 1238/1242 Å	C IV 1548/1551 Å	He II 1640 Å	C II 1335/1336 Å	Si II 1808/1820 Å	Comment
SWP37500A	2.6913	0.326	2.97	5.15	1.71	4.31	1.70	
SWP37500B	2.7188	0.344	2.42	6.20	1.30	5.30	1.93	
SWP37501A	2.7810	0.384	3.19	9.45	1.82	5.83	2.21	Flare?
SWP37501B	2.8100	0.402	2.58	7.60	1.30	5.52	1.93	
SWP37502A	2.8685	0.440	2.37	7.14	2.41	5.51	2.43	
SWP37502B	2.8965	0.458	1.79	5.87	1.74	4.93	1.20	
SWP37503A	2.9576	0.497	2.01	5.59	1.48	4.57	2.37	
Mean JD2			2.48(2.47)	6.71(6.26)	1.68(1.56)	5.14(5.02)	1.97(1.93)	
			±0.49(0.49)	1.47(0.94)	0.38(0.42)	0.55(0.51)	0.43(0.45)	
SWP37506A	3.4511	0.813	1.62	5.65	1.69	4.37	1.36	
SWP37506B	3.4789	0.831	2.15	11.92	1.58	6.50	2.30	Flare
SWP37509A	3.7313	0.992	3.07	7.67	1.90	4.23	2.28	
SWP37509B	3.7654	0.014	1.54	6.46	1.46	3.91	2.17	
SWP37511A	3.9389	0.125	1.54	3.49	0.98	1.78	0.97	
SWP37511B	3.9843	0.154	1.18	3.99	0.86	2.75	1.17	
Mean JD3			1.85(1.79)	6.53(5.45)	1.41(1.38)	3.92(3.41)	1.71(1.59)	
			±0.67(74)	3.06(1.73)	0.41(0.45)	1.61(1.11)	0.61(0.60)	
SWP37513A	4.2549	0.328	1.87	5.47	1.39	4.07	1.91	
SWP37513B	4.2858	0.347	2.93	13.47	3.63	7.36	4.24	Flare
SWP37514A	4.3355	0.379	2.09	5.35	2.00	4.86	1.96	
SWP37514B	4.3780	0.407	2.33	8.77	1.91	6.68	3.06	
SWP37515A	4.4433	0.448	2.54	6.41	1.47	4.83	1.78	
SWP37515B	4.4767	0.470	2.10	7.85	2.09	6.35	2.25	
SWP37516A	4.5457	0.514	1.96	5.96	1.23	4.64	1.91	
SWP37516B	4.5770	0.534	1.52	5.24	1.31	4.35	2.14	
Mean JD4			2.17(2.06)	7.32(6.44)	1.88(1.63)	5.39(5.11)	2.41(2.14)	
			±0.43(0.33)	2.79(1.37)	0.78(0.36)	1.22(1.00)	0.84(0.43)	
Overall Mean			2.18(2.08)	6.89(6.10)	1.68(1.57)	4.89(4.61)	2.06(1.92)	
			±0.56(0.52)	2.42(1.34)	0.58(0.40)	1.29(1.14)	0.70(0.51)	

2.4. EUVE *Fluxes*

CC Eri was observed by the Extreme Ultraviolet Explorer (EUVE) in September 1995 (Bowyer & Malina 1991). The observations were carried out with the Deep Survey/Spectrometer (DS/S) assembly for ≈ 160 ksec. The EUVE data were analyzed and corrected for instrumental effects using the IRAF-based EUV software EGOCS 1.6 and EGODATA 1.11 (Miller & Abbott 1995). Further analysis of the extracted spectra was carried out using the DIPSO package. Emission line fluxes were determined by fitting gaussians to the observed line profiles. The fluxes were corrected for interstellar attenuation assuming a mean hydrogen density of 0.05 cm^{-3} resulting to a column density of $\sim 2\times10^{18}$ atoms cm^{-2} at the distance of CC Eri (Zombeck 1990). The choice of this column density for CC Eri is in agreement with the database of column densities of Fruscione et al. (1994). Given the proximity of the source, a factor of two uncertainty in the hydrogen column density will only produce a 16% uncertainty in the line fluxes.

3. Results

3.1. Contemporaneous optical photometry

The SAAO and ESO data are given in Table 1 while the resulting light and colour curves are shown in Fig. 3.

From the data it was obvious that there were some small differences in the transformations and zero-point corrections between the two datasets, which could have been made worse by the use of two different comparison stars. Therefore, and since it was not possible to directly compare the mean colours of the star at these two observing runs, we shifted the SAAO data by 0.01 magnitudes in $(U–B)$, 0.025 in $(V–R)_c$ and 0.005 in $(V–I)_c$, with no correction in $(B–V)$. These shifts result when we compare the V light curves, which in both datasets have the same values either at phase 0.15 or phase 0.50, and we require the star to have at these phases for both datasets the same $(U–B)$, $(V–R)_c$ and $(V–I)_c$ colours respectively.

Table 3. IUE LWP emission line fluxes at Earth for CC Eri between 2–4 November 1989. A mean flux and associated variances are given for each line on each date. Phases are according to the ephemeris $2\,447\,129.5293 + 1.56145E$. The notation JD2, JD3 and JD4 refer to data taken on 2 Nov., 3 Nov. and 4 Nov. respectively.

IUE Image Number	JD 2 447 830.0+	Phase	Line Flux ($\times 10^{-13}$ erg s^{-1} cm^{-2}) Mg II 2796/2803 Å	Fe II 2600 Å	Comment
LWP16719A	2.6628	0.3080	42.00	1.46	
LWP16719B	2.6779	0.3177	41.38	1.40	
LWP16720A	2.7612	0.3710	40.69	1.46	
LWP16720B	2.7690	0.3760	43.44	1.27	
LWP16721A	2.8529	0.4298	45.49	1.67	
LWP16721B	2.8590	0.4337	46.61	0.88	
LWP16722A	2.9417	0.4866	42.51	1.01	
LWP16722B	2.9479	0.4906	44.33	1.56	
Mean JD2			43.31	1.34	
			$\pm$ 1.92	0.25	
LWP16727A	3.5216	0.8580	31.16	1.27	
LWP16727B	3.5282	0.8622	30.40	1.04	
LWP16730A	3.8163	0.0468	34.29	1.15	
LWP16730B	3.8238	0.0516	32.34	1.01	
Mean JD3			32.05	1.18	
			$\pm$ 1.47	0.10	
LWP16734A	4.3187	0.3685	49.74	1.38	Post-flare?
LWP16734B	4.3271	0.3739	46.62	1.61	
LWP16735A	4.4054	0.4240	47.37	1.49	
LWP16735B	4.4135	0.4292	48.38	1.13	
LWP16735A	4.5103	0.4912	53.27	1.20	
LWP16736B	4.5179	0.4961	49.37	1.88	
LWP16737	4.6055	0.5522	44.99	1.47	
Mean JD4			48.53	1.45	
			$\pm$ 2.54	0.23	
Overall mean			42.86	1.33	
			$\pm$ 6.39	0.25	

Table 4. The CC Eri flare line fluxes at Earth.

IUE Image Number	JD 2 447 830.0+	Phase	Line Flux ($\times 10^{-13}$ erg s^{-1} cm^{-2}) N V 1238/1242 Å	C IV 1548/1551 Å	He II 1640 Å	C II 1335/1336 Å	Si II 1808/1820 Å
SWP37501A	2.7810	0.384	0.72	3.19	0.26	0.61	0.28
SWP37506B	3.4789	0.831	0.36	6.47	0.20	3.09	0.71
SWP37513B	4.2858	0.347	0.87	7.03	2.00	2.25	2.10

There is a slight evolution between the SAAO data (and probably also within it) and the ESO data taken almost a month later. A low amplitude modulation is visible in V with a peak-to-peak variation of ~ 0.035 and a mean value of 8.764 for the SAAO curve. These data show, within the errors of the photometry, no modulation in $(B–V)$ and $(V–R)_{\rm c}$ and only small variations in $(V–I)_{\rm c}$ weakly correlated with the light curve. The largest variation, larger than the intrinsic errors of the photometry, is present in the $(U–B)$ colour with an amplitude of ~ 0.05 mag. The ESO data, taken one month later, appear brighter in V than the SAAO data. The double-peaked V light curve shows an amplitude of ~ 0.040 with a mean value of 8.757 and the colour curves are clearly correlated with it, although their amplitudes are very small.

3.2. Orbit and system parameters

Radial velocities have been determined from Ca II H and K for the primary and secondary components of the binary using the task FXCOR within IRAF. The spectra were cross-correlated with one of the spectra taken on November 4, which had a high signal-to-noise ratio, as no radial velocity standards were observed. The velocity residuals for the primary measurements are of the order of $\sim$ 2 km s^{-1} and up to 8 km s^{-1} for the

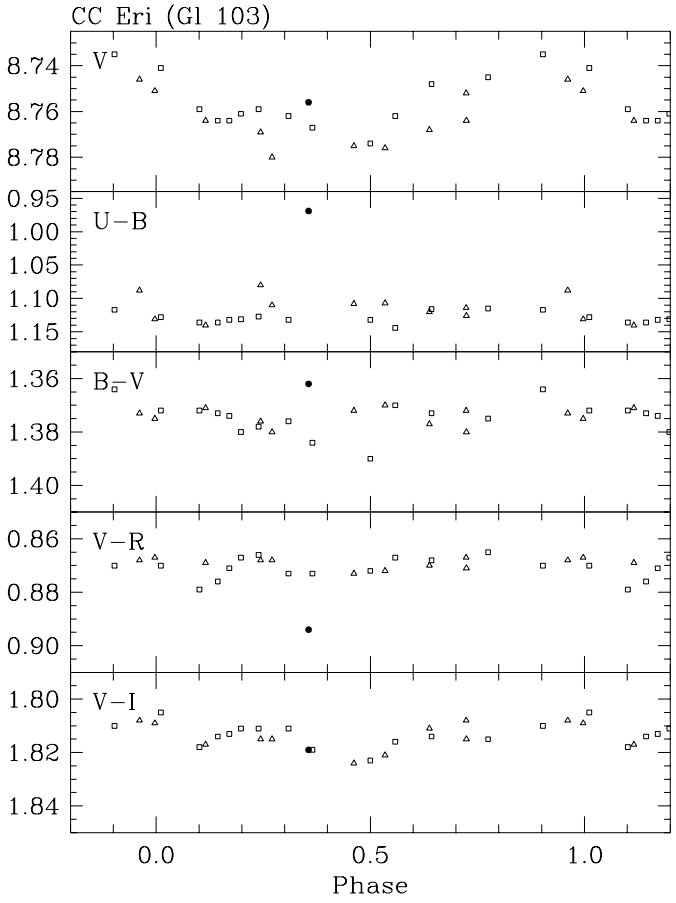

Fig. 3. Light and colour curves for CC Eri based on SAAO data taken between 3–10 November 1989 (*triangles*) and ESO data taken 9–28 December 1989 (*squares*). The filled circles indicate the point which records the flare of 4 November. Phases are those from Table 1.

Table 5. The orbital solution for CC Eri of Evans (1959) compared with the present results.

	Evans	Present work
Period (d)	1.56145	1.5615
γ (km s^{-1})	+41.94	–
$K_{\rm p}$ (km s^{-1})	37.77	37.185
$K_{\rm s}$ (km s^{-1})	–	69.289
ω	63.°8	–
e	0.0461	0.0
$a_{\rm p} \sin i$ (km)	$8.100\,10^5$	$7.984\,10^5$
$a_{\rm s} \sin i$ (km)	$15.71\,10^5$	$14.878\,10^5$
$m_{\rm p}/m_{\rm s}$	1.94	1.863
$m_{\rm p} \sin^3 i$	0.1462	0.1271
$m_{\rm s} \sin^3 i$	0.0753	0.0682

secondary. These residuals were used as standard errors in the weighting of the least-square orbital fit.

We obtained a preliminary orbital solution, using Evans (1959) orbit as a first guess. Fixing his value for the velocity of the centre of mass of the system γ, resulted in a value for the orbital period of $P = 1.54539 \pm 0.00171$ days (the eccentricity was fixed equal to 0). If we add Evan's data to enlarge

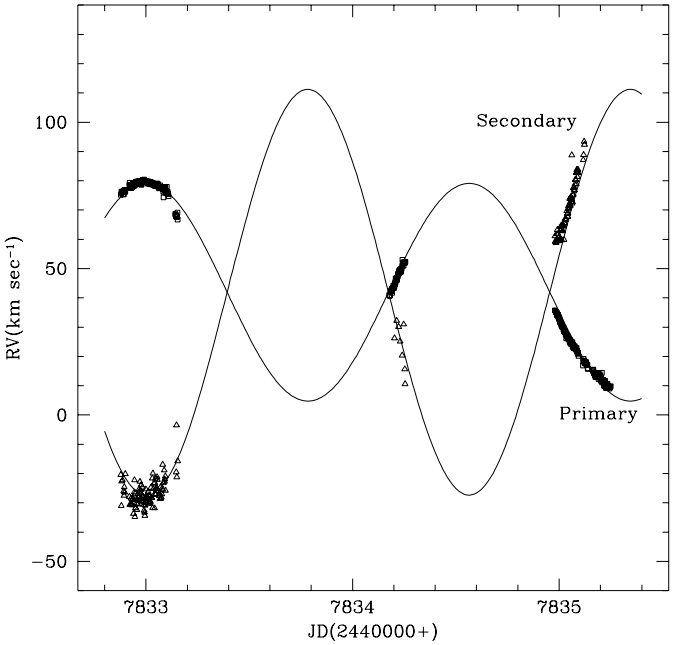

Fig. 4. Measured radial velocities for CC Eri and its companion along with the orbital solution mentioned in the text (triangles indicate the secondary while square indicate the primary).

the time baseline and, thus, improve the fit, we obtain a period of $P = 1.5615$ days. This is the value for the period we have used in the calculations of the minimum masses ($M \sin^3 i$) and separations given in Table 5, where we compare Evans' solution with our own. The radial velocity data are plotted in Fig. 4 with our orbital solution. The mass function of the system is

$$\frac{m_{\rm s}^3 \sin^3 i}{(m_{\rm p} + m_{\rm s})} = 8.319\,10^{-3},$$

where $m_{\rm p}$ and $m_{\rm s}$ are the masses of the primary and secondary respectively.

3.3. Emission line fluxes

Line fluxes from Tables 3 and 4 are plotted in Figs. 5 and 6 against phase, where this has been computed from the ephemeris JD$= 2\,447\,129.5293 + 1.5615E$. It is readily apparent that these line fluxes are variable. The data cover phase intervals of $\Delta\phi \approx 0.179$ on JD2 (2 Nov), 0.193 on JD3 (3 Nov) and 0.184 on JD4 (4 Nov). Due to the almost day and a half orbital period of the system, the third data set coincided in phase with the first one.

It will also be noted from Tables 2 and 3 that the flux of all the emission lines is systematically lower on JD3 than on either of the other dates. This is most obvious in the case of the Mg II lines but it can also be seen throughout. Even at the same phases, there is evidence, at least in the Mg II fluxes, of a change in the mean level after only two rotations (from JD2 to JD4). The mean Mg II line flux at Earth is approximately $4.3\,10^{-12}$ erg s^{-1} cm^{-2}, comparable to that found in 1979 by Byrne et al. (1982) and that of the C IV line is $\approx 6.1\,10^{-13}$ erg s^{-1} cm^{-2}, excluding the two flare points.

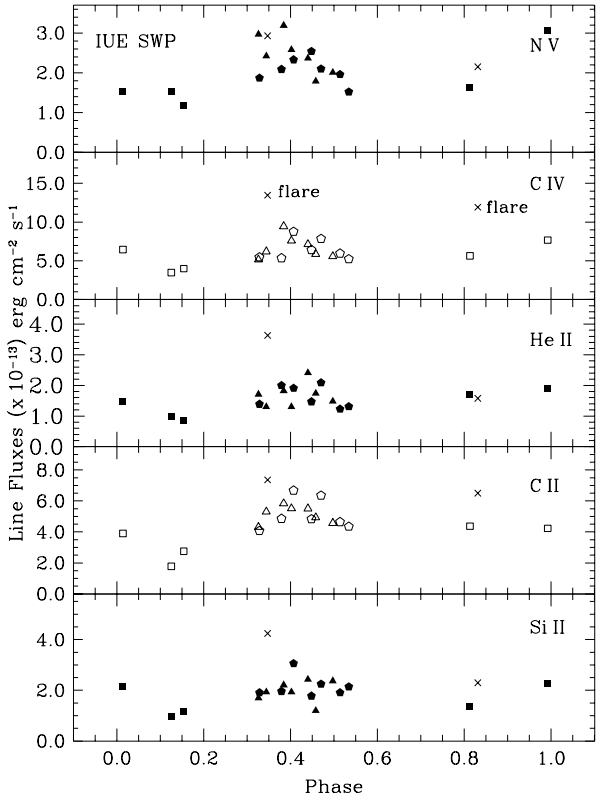

Fig. 5. IUE SWP emission line fluxes versus phase. From top to bottom, N V, C IV, He II, C II and Si II line fluxes plotted against phase. Triangles represent the data taken on 2 Nov, squares on 3 Nov and pentagons on 4 Nov.

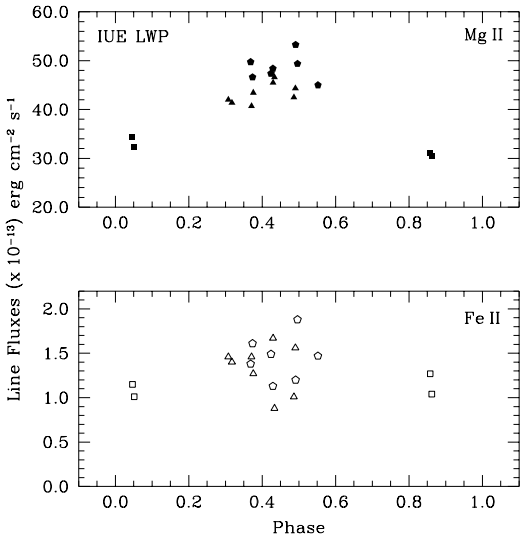

Fig. 6. IUE LWP emission line fluxes versus phase. The Mg II (upper panel) and Fe II line fluxes (lower panel) are plotted against phase. Symbols are as in Fig. 5

There is no clear evidence of a systematic behaviour of the line fluxes with phase, partly due to the gaps in coverage, but there is a much larger scatter in the individual measurements of the Mg II flux than would be expected from measurement errors alone ($\approx 10\%$). The only feature that seems to repeat in the flux curve is a dip in the flux of the Fe II lines, which can be seen at $\phi \approx 0.45$ for both the JD2 and JD4 data.

3.4. Flares

The C IV (λ1548/1551 Å) line, the strongest in the SWP spectra (after Ly α), has two widely discrepant points. The first of these is at phase 0.347 on JD4, while the second is at phase 0.831 on JD3. This C IV flux increase on JD4 is also seen in virtually all of the other prominent lines. That on JD3 is only obvious in C II. These were two discrete flares, marked as such in the C IV line flux plot (Fig. 5). The corresponding points in the C II and Si II line fluxes are also marked.

4. Discussion and conclusions

4.1. Physical parameters of the binary system from the orbital solution

Before we can determine surface line fluxes, we must determine a value for the radii of the two components of the system. If we take the spectral type of the primary as K7.5Ve and its mass (Schmidt-Kaler 1982) as 0.57 $M_\odot$, then the companion is of mass 0.306 $M_\odot$ or spectral type M3.5Ve. The radii are (Schmidt-Kaler 1982) $R_{\rm P} = 0.645$ $R_\odot$ and $R_{\rm S} = 0.41$ $R_\odot$. Using the effective temperature, $T_{\rm eff}$ and the visual absolute magnitude, M_V, Głębocki & Stawikowski (1995) inferred a radius of $R = 0.61$ $R_\odot$. The spectral types match those derived from the colours for another epoch (K7V + M3V) by Cutispoto (1998).

Pettersen (1983) gave a $v_{\rm rot}$ of 19.8 km s^{-1}, which yields a radius of $R_{\rm P} = 0.61$ $R_\odot$. Bopp & Evans (1973) assumed a $v \sin i$ of ~ 15, which yielded a minimum radius of $R_{\rm P} \sin i = 0.46$ $R_\odot$.

The mean flux ratio at Earth $F_{\rm P}$(Ca H)/$F_{\rm S}$(Ca H) on 2 Nov was measured as 2.6. Assuming the radii as derived above, the ratio of the areas, $(R_{\rm P}/R_{\rm S})^2 = 2.47$. Thus, within the errors, the Ca H brightness of the components is similar.

4.2. Spot distribution

Comparing the photometric data of CC Eri taken before and after this observing run (Cutispoto 1991, 1992; Cutispoto & Leto 1997), it can be readily seen that the star was in the process of becoming brighter; in fact, almost a year later (in September 1990) it reached the brightest maximum ever observed, namely, $V = 8.70$ magnitudes (Cutispoto & Leto 1997), which is even brighter than the $V = 8.71$ observed in late 1958 by Evans (1959). Phillips & Hartmann (1978) reported photographic magnitudes from the Harvard plate collection of CC Eri and found a value for the B filter at maximum brightness of $B_{\rm max} = 10.03$. If we calculate the corresponding $B_{\rm max}$ for the 1990 epoch (Cutispoto & Leto 1997), we obtain $B_{\rm max} = 8.70 + 1.35 = 10.05$, which is, within the errors of the photographic measurements, the same as the maximum given by Phillips & Hartmann (1978). That the star was near its

Table 6. EUVE line fluxes in erg s^{-1} cm^{-2}

Spectral line	Flux
Fe XVIII 93.92 Å	$1.1\ 10^{-13}$
Fe XIX 108.37 Å	$1.0\ 10^{-13}$
Fe XX/XXIII 132.85 Å	$1.9\ 10^{-13}$
He II 304 Å	$8.5\ 10^{-13}$

unspotted magnitude together with the very small amplitudes we measured in the light and colour curves, point towards the idea of a reduced coverage of spots at the 1989 epoch.

The fact that the mean V magnitude was fainter in the SAAO data than for the ESO data (taken one month later) could be explained by the star becoming brighter towards its historical maximum. The large intrinsic variation of the (U–B) SAAO data could be explained by the appearance of hotter, brighter material on the atmosphere of one of the stars (e.g. a flare or plages), which could produce temporary bluer ultraviolet colours (Amado & Byrne 1997). This scenario coincides with the flaring state at which the star was during the SAAO observations.

4.3. Ultraviolet line fluxes and evidence for rotational modulation

The individual flux measurements of the Mg II resonance lines give some small evidence of a modulation in anti-phase with the optical variation. This would perhaps confirm earlier results that chromospheric emission is correlated in a general sense with optical spots. However, the lesser modulation of the broadband optical illustrates that the area coverage in the two are not related on a one-to-one basis.

Comparing the line flux variations with the broadband V light curves, we note that the contrast in the Mg II (max-to-min) is much larger, $\approx 40\%$, than in V, $\approx 5\%$. The evidence for modulation of the higher temperature lines, i.e., Si II, C II and C IV resonance lines, is much weaker. Any variation here is dominated by intrinsic variations, which are $\approx 50\%$, much greater than typical errors of measurement ($\approx$ 10–20%).

The lack of detectable modulation in C IV due to the presence of a large scatter, possibly due to low level flaring, is in keeping with previous results for the stars BY Dra and AU Mic (Butler et al. 1987).

4.4. Emission measure and quiescent radiative losses

Based on the IUE and EUVE lines fluxes of Table 2 and Table 6 respectively, an emission measure (EM) curve (see Fig. 7) can be constructed using the atomic data as given in Doyle & Keenan (1992a) and Brickhouse et al. (1995). Then from the adopted EM curve (this is actually a set of loci which give upper limits to the actual EM distribution), we can estimate the total radiative losses from the upper chromosphere to the corona (i.e. over the temperature range $4.1 < \log T_e < 7.1$) by multiplying the EM by the radiative loss function. Here, we used the radiative

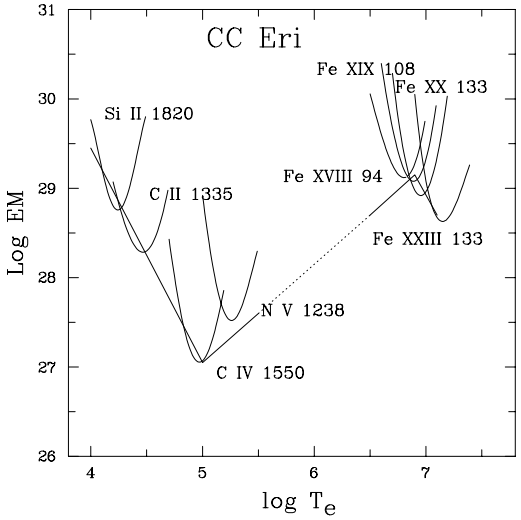

Fig. 7. The emission measure curve for CC Eri based on the IUE and EUVE data in Tables 2 and 6 respectively. Note the data gap between $\log T_e = 5.5$ and 6.5.. see text.

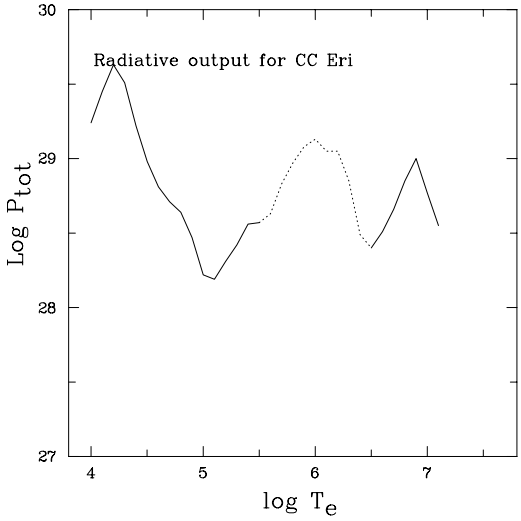

Fig. 8. The radiative losses (in erg s^{-1}) from the chromosphere, transition region and corona of CC Eri as a function of $\log T_e$. The region between $\log T_e = 5.5$ and 6.5 is uncertain due to the lack of spectral lines and its shape here is dominated by the shape of the radiative loss function.

cooling curves of Cook et al. (1989). Brickhouse et al. give the split of the line at 133 Å as 33% Fe XX, 67% Fe XXIII assuming a constant EM. However, such a divide implies the Fe XX point significantly below that of Fe XIX. For the EM points as given in Fig. 7 we adopted a 50:50 split. Due to the lack of lines, particularly in the mid-to-upper transition region, we simply fitted a series of linear fits for the outline of the assumed EM curve. The correct shape of the EM curve in this temperature region is therefore unknown. From these fits we estimate surface radiative losses of $\sim 5.6\ 10^7$ erg s^{-1} cm^{-2} in quiescent, giving total losses over the whole surface of $2.9\ 10^{30}$ erg s^{-1}. The total radiative losses as a function of temperature is shown in Fig. 8, the shape of this figure is largely dominated by the radiative loss

function, although the second high temperature peak reflects the 10^7 K coronal temperature of CC Eri. In the construction of the EM curve we used the HIPPARCOS distance of 11.51 pc and a stellar radius of $0.65 R_\odot$, i.e. we assumed the emission was from the K star.

An alternative method of obtaining an estimate of the total radiative losses (chromospheric, transition region and coronal) is to use a relationship derived by Bruner & McWhirter (1988) between the total radiated power in a hot plasma and the power radiated in specific spectral lines, e.g. C IV 1550 Å or N V 1240 Å. For the quiescent state we get $2.1\ 10^{30}$ erg s^{-1} (from C IV), in excellent agreement with that estimated via the EM technique.

4.5. Flares

The two flares radiated $2.7\,10^{31}$ erg and $1.6\,10^{31}$ erg in the C IV 1550 lines alone. These are large flares by the standards of IUE observations of dMe stars and are several orders of magnitude larger than solar two-ribbon flares. Using the scaling between the C IV radiative output and the total flare radiative output derived for solar flares by Bruner & McWhirter (1988) we estimate the energy radiated over the entire outer atmosphere ($4.1 \leq \log T \leq 8.0$) of these flares to be each $\approx 10^{36}$ erg.

Van den Oord (1988) showed that for a two-ribbon flare involving a filament of length l, the maximum amount of energy stored is given by

$$W = 1.6\,10^{37} \left(\frac{l}{R_\odot}\right) \left(\frac{R_*}{R_\odot}\right)^2 \left(\frac{B_{\rm surf}}{1000\,{\rm G}}\right)^2 \ {\rm erg} \qquad (1)$$

where $B_{\rm surf}$ is the surface magnetic field strength at the star. Taking $R_* = 0.65\,R_\odot$ and a filament length of $\sim 0.2\,R_\odot$ (i.e a quarter of the stellar radii) implies kilo-gauss fields on CC Eri. Since this however assumes a very high magnetic energy conversion rate, these larger super-flares could therefore be the result of the magnetic fields in the two stars interacting. For example, van den Oord (1988) showed that for a binary the maximal storage of energy is obtained when the filament is located between the two components. In this case the binary nature allows storage of a factor of $(1.6\,a/R_*)^2$ more energy (where a is the binary separation), implying at least an order of magnitude more energy available than for a single star. Such an interpretation has being applied to flares on RS CVn binaries (Doyle et al. 1992b).

Acknowledgements. Research at Armagh Observatory is grant-aided by the Department of Education for N. Ireland. This work used computer hardware and software provided by the UK Starlink Project which is funded by the UK PPARC. PJA acknowledges financial support from Armagh Observatory, and Catania Astrophysical Observatory, and computing and technical support from the Instituto de Astrofísica de Andalucía. Our work was based on observations made with the International Ultraviolet Explorer satellite at the ESA Satellite Tracking Station, Vilspa, Spain, and at the NASA Goddard Space Flight Center, Maryland, USA and on observations from the Anglo Australian, South African Astronomical Observatory and European Southern Observatory. We acknowledge the contribution of Dr. P.M. Panagi to this paper. A lot of this work could not have been achieved without the effort and determination of our late colleague Brendan Byrne who's untimely death occurred before this paper was completed.

References

Amado P.J., Byrne P.B., 1997, A&A 319, 967
Bopp B.W., Evans D.S., 1973, MNRAS 164, 343
Bowyer S., Malina R.F., 1991, In: Malina R.F., Bowyer S., Extreme Ultraviolet Astronomy, Pergamon Press, p. 397
Brickhouse N.S., Raymond J.C., Smith B.W., 1995, ApJS 97, 551
Bromage G.E., 1984, in: European IUE Conf., p. 473
Bruner M.E., McWhirter R.W.P., 1988, ApJ 326, 1002
Busko I.C., Torres C.A.O., 1976, IAU Comm. 27 Inf. Bull. Var. Stars No. 1186
Butler C.J., et al., 1987, A&A 174, 139
Byrne P.B., Butler C.J., Andrews A.D., 1982, Irish Astron. J. 14, 219
Byrne P.B., Cutispoto C., Kilkenny D.W., Neff J.E., Panagi P.M., 1992, in: Byrne P.B., Mullan D.J. (eds.), Surface Inhomogeneities on Late-Type Stars, Springer, p. 255
Caillault J.-P., Drake S., Florkowski D., 1988, AJ 95, 887
Cook J.W., Cheng C.-C., Jacobs V.L., Antiochos S.K., 1989, ApJ 338, 1176
Cutispoto G., 1991, A&AS 89, 435
Cutispoto G., 1992, A&AS 95, 397
Cutispoto G., 1995, A&AS 111, 507
Cutispoto G., Leto G., 1997, A&AS 121, 369
Cutispoto G., 1998, A&AS 127, 207
Doyle J.G., Keenan F.P., 1992a, A&A 264, 173
Doyle J.G., van den Oord G.H.J., Kellett B.J., 1992b, A&A 262, 533
Evans D.S., 1959, MNRAS 119, 526
Fruscione A., Hawkins I., Jelinsky P., Wiercigroch A., 1994, ApJS, 94, 127
Giddings J., 1983, IUE ESA Newsletter 17, 53
Głębocki R., Stawikowski A., 1995, Acta Astron. 45, 725
Howarth I.D., Murray J., 1988, STARLINK User Note 50, 10
Jefferies R.D., Byrne P.B., Doyle J.G., et al., 1994, MNRAS 270, 153
Menzies J.W., Cousins A. Banfield R.M., Laing J.D., 1989, S. Afr. Astr. Obs. Circ. 13, 1
Miller A., Abbott, M., 1995, EUVE Guest Observer Software, Version 1.5
Pallavicini R., Monsignori-Fossi B.C., Landini M., Schmitt J.H.M.M., 1988, A&A 191, 109
Pallavicini R., Tagliaferri G. & Stella L., 1990, A&A 228, 403
Pan H.C., Jordan C., 1995, MNRAS 272, 11
Pettersen B.R., 1983, in: Byrne P.B., Rodonò M. (eds.), Activity in red-dwarf stars, Dordrecht: D. Reidel Publishing Co. p. 17
Phillips M.J., Hartmann L., 1978, ApJ 224, 182
Schmidt-Kaler T., 1982, 2b, Landolt-Börnstein, Heidelberg: Springer
Schmitt J.H.M.M., Pallavicini R., Monsignori-Fossi B.C., Harnden F.R.J., 1987, A&A 179, 193
Tody D., 1986, in: D. Crawford (ed.), Instrumentation in Astronomy VI., Proc. SPIE p. 733
Tsikoudi V., 1988, AJ 95, 1797
van den Oord G.H.J., 1988, A&A 205,167
White S.M., Lim J., Kundu M.R., 1994, ApJ 422, 293
Zombeck M.V., 1990, In: Handbook of Space Astronomy & Astrophysics, Cambridge University Press